Publishing House
AKAPIT

COMPUTER METHODS IN MATERIALS SCIENCE
Informatyka w Technologii Materiałów

Vol. 15, 2015, No. 3

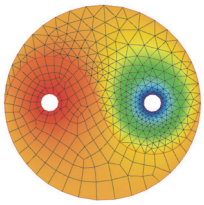

STRUCTURAL EVOLUTION AND MECHANICAL PROPERTIES CHANGES IN DUAL-PHASE STEEL DURING CONTINUOUS ANNEALING PROCESS

ROMAN KUZIAK[1], KRZYSZTOF RADWAŃSKI[1], WŁADYSŁAW ZALECKI[1], ARTUR MAZUR[1], ANDRZEJ WROŻYNA[1], NORBERT KWIATON[2], JEAN CHRISTOPHE HELL[3], JEAN-LOUIS COLLET[4]

[1] *Instytut Metalurgii Żelaza, ul. K. Miarki 12-14, 44-100 Gliwice, Poland*
[2] *Salzgitter Mannesmann Forschung GmbH*
[3] *ArcelorMittal Maizières Research SA*
[4] *Centre de Recharches Metallurgiques*
**Corresponding author: rkuziak@imz.pl*

Abstract

The paper presents the results of the investigation aimed at detailed characterisation of the changes occurring in the microstructure of cold rolled DP steel in the continuous annealing/galvanizing process. These changes include static recrystallization of ferrite and transformation of initial ferritic – pearlitic microstructure into ferrite and austenite during heating stage and reverse transformation of austenite into ferrite and next into martensite + bainte during cooling stage of the continuous annealing/galvanizing process. It was found that the static recrystallization of ferrite during heating starts at around 600°C whilst the transformation of ferrite + pearlite to austenite + ferrite starts at around 750°C. The kinetics of phase transformation during cooling depends on the peak temperature of the thermal profile. If this temperature is within two – phase range, no nucleation process is involved in ferrite nucleation and the transformation of austenite into ferrite begins almost instantaneously after start of cooling. On the contrary, nucleation process occurs when the cooling is applied from the temperature of austenite stability. This results in the undercooling of austenite with respect to the Ae3 temperature which depends on the cooling rate. Further transformation of remaining austenite into low temperature transformation products (bainite and martensite) is dependent on the hardenability of particular DP steel and cooling rates applied. However, in real industrial process, cooling conditions should be carefully controlled due to the limitations of galvanizing operation. This imposes limits on the cooling rates, and generally leads to the decomposition of austenite into martensite and bainite mixture instead of martensite alone. The physical simulation of continuous annealing using Gleeble 3800 simulator showed a strong dependence of the microstructure and mechanical properties of DP steel strips on peak temperature and soaking time as well as on tempering temperature and time.

Key words: DP steels, continuous annealing/galvanizing, phase transformations, microstructure, mechanical properties

1. INTRODUCTION

Mechanical properties of DP steels are mainly connected with hard constituents (martensite and bainite) volume fraction in their microstructure. Although the dependence of strength and ductility of DP steels on martensite content is well described in technical literature, there are a lot of technological and functional properties of these steels depending on discrete microstructural features that are not subject to standard examination. For example, it has been reported that the crashworthiness of DP steels increases as the degree of refinement of martensite island increases, which can be characterised by ferrite-martensite perimeter (Krebs et al., 2010). Other features of DP steel microstructure that are not subject to routine investigation include contiguity, continuity and microstructural bending (Aarnst, 2009).

ISSN 1641-8581

These quantifiable microstructure characteristics have a substantial effect on the in use properties, as well as on functional performance of DP steels. The literature data concerning the effect of these parameters on mechanical and functional properties of DP steels are rather scarce. Typically, the strength properties of these steels are correlated with martensite volume fraction, ferrite grain size or ferrite mean-free distance (Calcagnotto et al., 2009; Kuziak et al., 2008; Bag et al., 1999). The most advanced model including the effect of "soft" ferrite and hard particles of martensite is described by Radwański et al. (2015).

Beyond the chemical composition, the mechanical and functional properties of DP steels are influenced by many factors/parameters, pertaining to continuous casting, hot and cold rolling, and finally, thermal profile parameters during continuous annealing/galvanizing. Due to the complex effect of the continuous annealing/galvanizing thermal profile parameters, a required balance of the properties of the strips can be achieved by properly adjusting the most influencing process parameters to the specific product requirements.

This paper presents experimental results obtained during VADPsheet project realisation (Kuziak, 2015). The main aim of the project was to develop a robust model and implement it in the form of the computer software capable of predicting the explicit picture of the microstructure and mechanical properties of DP thin strips subject to continuous annealing/galvanizing process. The results will comprise the characterisation of metallurgical changes occurring in the microstructure of continuously annealed cold rolled strips to produce DP structure that are schematically superimposed on the general thermal profile of continuous annealing/galvanizing process in figure 1.

The metallurgical changes characterised in figure 1 were described in this paper with relevance to the heating/soaking and cooling stage of the continuous annealing process. The most important changes occurring at the heating/soaking stage include ferrite recrystallization and transformation of initial microstructure of deformed ferrite and pearlite into austenite. During cooling stage, the first transformation that must be carefully controlled is ferrite transformation. The ferrite transformation causes carbon segregation into remaining austenite which is crucial for further transformation of this phase during cooling to ambient temperature.

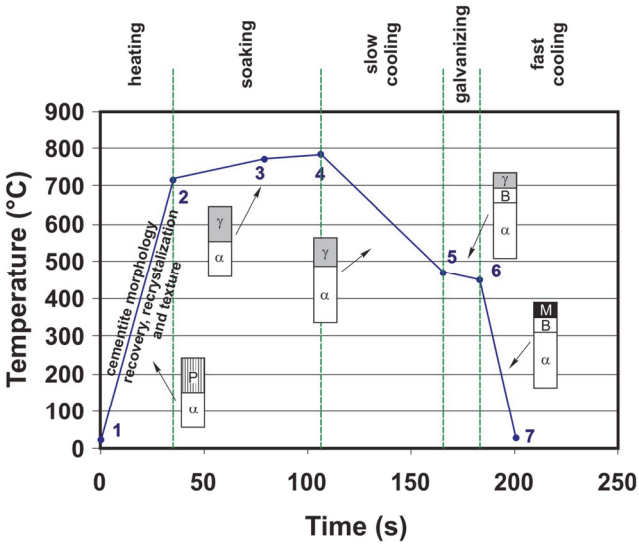

Fig. 1. *Metallurgical changes occurring in the cold rolled strip subject to continuous annealing/galvanizing thermal profile*

2. MATERIAL AND EXPERIMENRAL METHODOLOGY

The results obtained in VADPSheet project are presented for one laboratory heat that was cast in vacuum furnace into 70-kg ingot. Chemical composition of the heat is given in table 1.

The ingot of experimental steel was forged into bars having 45x45mm in cross section, and subsequently hot rolled on laboratory reversing mill into 2.9 mm thick steel strip. Prior to rolling, the bar was heated to 1220°C and held at this temperature for 30 minutes. The hot rolling was performed with 10 passes, and the finished rolling temperature (measured at the strip surface) was around 870°C. Following rolling, the strip was transferred to the furnace heated to temperature 650°C where it was subject to slow cooling to ambient temperature at a rate of around 40°C/hour, which simulated cooling of coiled strip. Next, after removing the surface oxide scale, cold rolling was conducted in several passes to produce strips having thickness of around 1 mm. The samples for the microstructure investigation

Table 1. *Chemical composition of experimental laboratory heat (wt.%)*

C	Mn	Si	P	S	Cr	Ni	Mo	Ti	N
0.09	1.42	0.10	0.011	0.010	0.35	0.01	0.02	0.001	0.0043

were subject to different thermal treatments in the DIL 805 A/D dilatometer and next in Gleeble 3800 thermal-mechanical simulator. The samples for dilatometric investigation have dimensions of 1 x 1 x 7 mm, whilst that for the continuous annealing simulations in Gleeble have dimensions of 1 x 50 x 250 mm. The experiments were conducted on the samples taken from the cold rolled material. The methodology and parameters of the dilatometric experiments were designed depending on the required information. In order to characterise the ferrite recrystallization and phase transformations, the samples were heated to defined temperatures in the range 550 - 900ºC at different rates. After reaching the targeted temperature, the samples were either fast cooled to ambient temperature or cooled after holding for times ranging from 10 to 3600 seconds. The results of the investigation provide the knowledge about the mechanisms and kinetics of ferrite recrystallization and phase transformation of initial microstructure to austenite + ferrite in two-phase region or directly to austenite above A_{c3} temperature. The experiments conducted in Gleeble 3800 simulator were aimed at identifying the effect of thermal profile parameters on microstructure and mechanical properties of DP strips.

The samples subject to different thermal cycles were investigated by means of scanning electron microscopy (SEM) and using EBSD analysis. Changes in the structure caused by holding at elevated temperatures were described qualitatively and

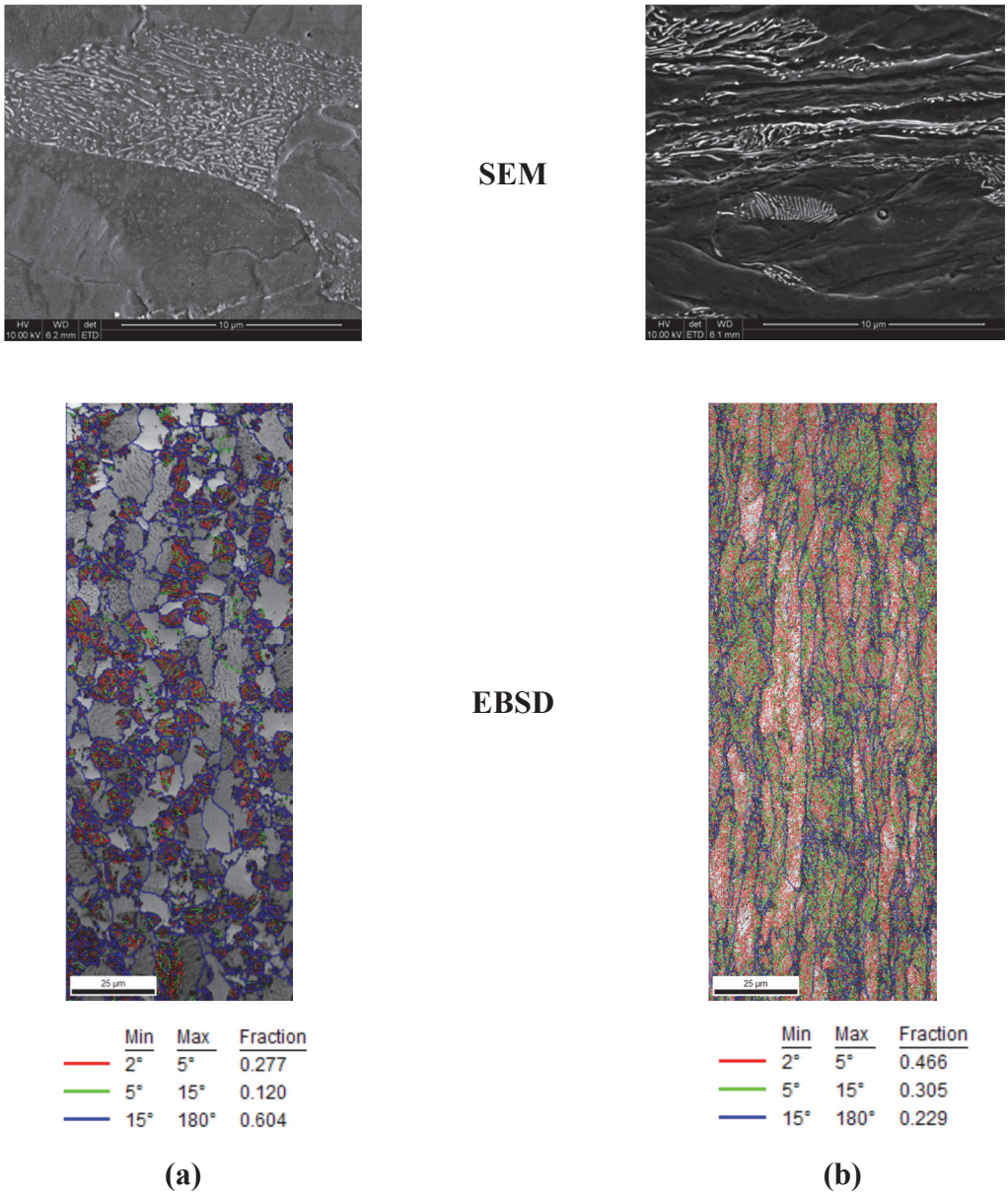

Fig. 2. *SEM and EBSD investigation of the structure of strip from experimental steel following hot rolling (a) and cold rolling (b)*

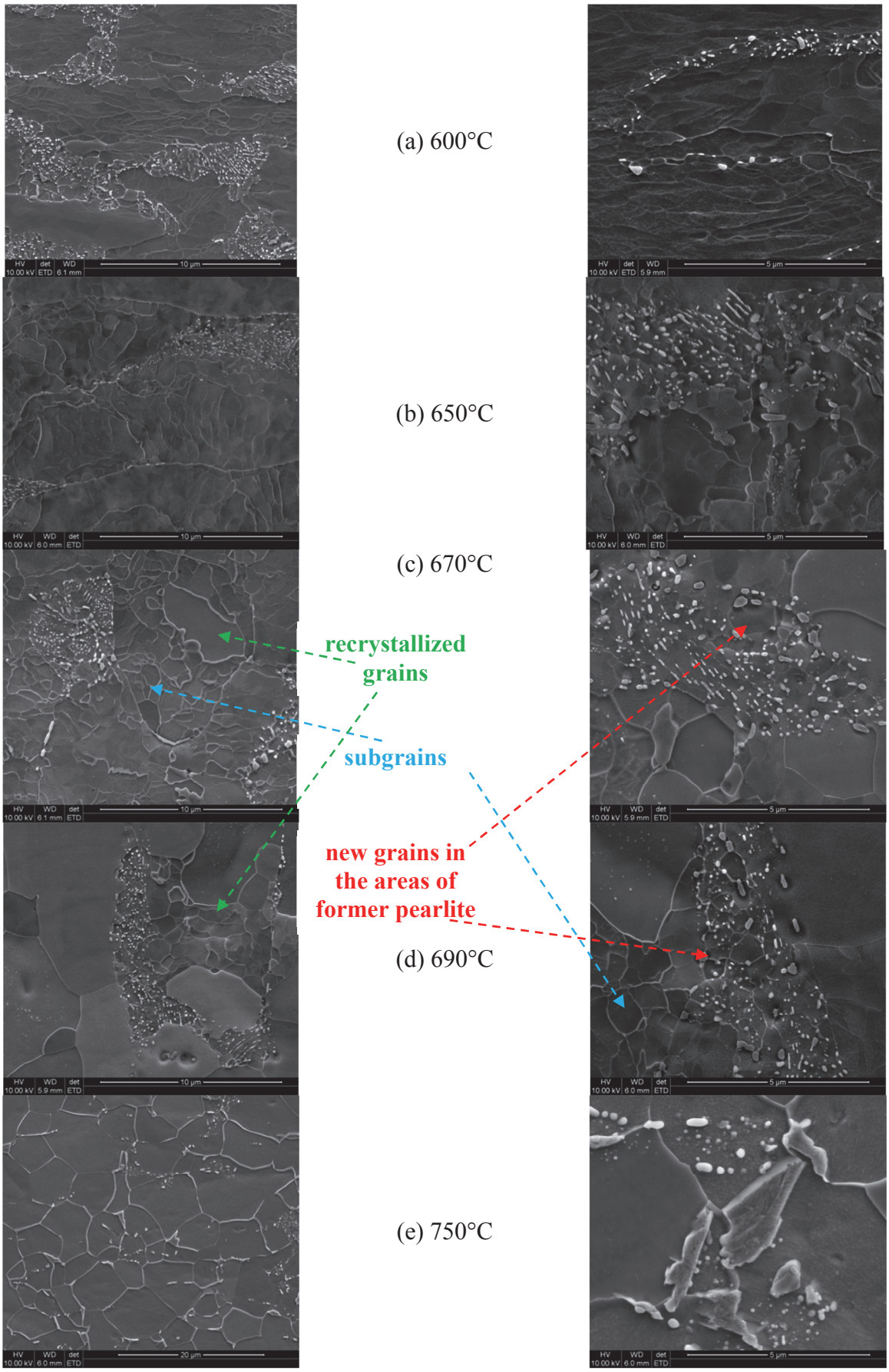

Fig. 3. *Evolution of the strip structure as function of temperature during heating at rate 3 °C/s, SEM*

quantitatively by means of parameters determined by EBSD analysis, including: Image Quality (IQ), Kernel Average Misorientation (KAM), Grain Average Misorientation (GAM) and Grain Orientation Spread (GOS). The methodology of these investigations was described in (Radwański, 2015; Radwański et al., 2015).

3. CHARACTERISATION OF THE METALLURGICAL CHANGES OCCURRING IN THE STRIP STRUCTURE DURING CONTINUOUS ANNEALING (CA)

3.1. Heating and soaking stage of CA process

The kinetics of microstructural changes occurring in the cold rolled strips during heating stage of thermal profile are dependent on the initial microstructure. This microstructure was investigated with scanning electron microscopy and EBSD technique, and the results are shown in figure 2b. For the sake of comparison, also the microstructure of the hot rolled plate is also shown in this figure 2a. The pictures of the microstructure were taken in the mid-thickness area. Microstructure of the hot rolled strip consists of ferrite and pearlite or degenerate pearlite (figure 2a). Cold rolling caused a strong elongation of ferrite grains and the development of deformation substructure inside the grains. The pearlite areas are deformed approximately to the same degree as the ferrite grains. However, the main features of the deformed substructure are clearly seen only in ferrite.

The micrographs in figure 3 show that the microstructure restoration processes in deformed ferrite grains started above approximately 600°C. Above this temperature the process of regular subgrains formation started in the grains interiors. At 650°C, the fragmentation process of cementite plates, and subsequent coagulation of fragmented particles in the areas of former pearlite is observed. The cementite coagulation process is controlled by the carbon diffusion process along grains boundaries which are the easy diffusion paths. The dissolution and coagulation process of cementite particles resulted in their redistribution along the grain boundaries. As a result of this mechanism, the particle distribution in the microstructure is following the subgrain/grain boundaries pattern. However, this process is strongly dependent on the heating rate. The time of fast heating to defined temperature is short and due to this the particles are gathered more closely in the area of their initial distribution. Slow heating leads to the expansion of the particles far away of the area of their initial location. In the former case, the final microstructure inherits to a greater extent the morphological features of the original microstructure than in the latter one. However, even at slow heating rates, some particles were captured inside the ferrite grains. Results of the EBSD investigation of the changes occurring in the microstructure during heating are shown in figure 4. The results of analysis of

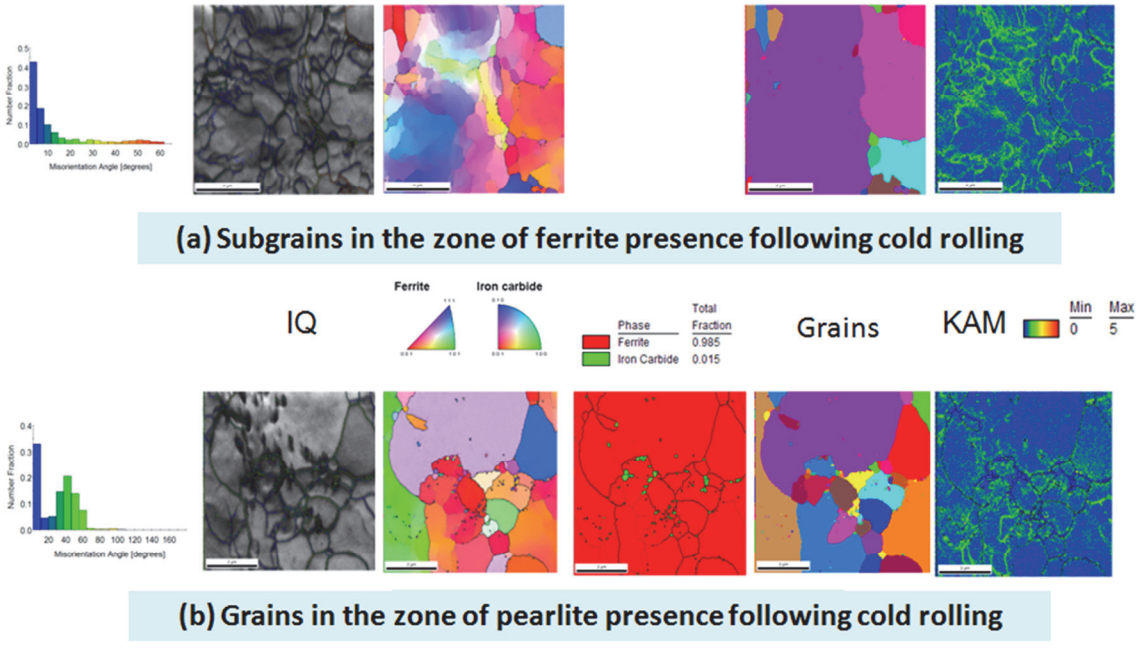

Fig. 4. *Results of EBSD investigation of the sample after heating to 670°C in the former region of (a) ferrite, (b) pearlite*

the ferrite area are shown in figure 4a, while figure 4b shows the area where initially pearlite was present. In the sample heated to 670°C, the formation of fine recrystallized ferrite grains is seen in the areas of microstructure characterized by severe local deformation. The dislocation rearrangement and formation of subgrains inside the ferrite grains is more advanced compared to lower temperatures. Also, the changes in crystallographic orientation inside grains characterized by KAM parameter are larger as compared to the recrystallized grains. Formation of small-size subgrains/grains and carbon redistribution and precipitation followed by the coagulation of cementite particles is observed in the regions formerly occupied by pearlite. During the fast cooling from the peak temperature, a substantial amount of new ferrite is formed, which is related to low hardenability of the investigated steel.

Microstructure of the sample is composed of deformed and recrystallized ferrite and partially transformed pearlite grains or cementite aggregates. In the gray scale picture of IQ in figure 5(a-b), the recrystallized ferrite grains are brighter as compared to pearlite regions and deformed ferrite grains. This can be related to higher value of IQ parameter presented in colour map and IQ distribution in figure 5(c-d). The IQ distribution map parameter with marked grain boundaries is shown in figure 5c. The IQ parameter is lower in the areas characterized by misorientation angles ≤15°. There are also neighbouring areas with misorientation angles ≤15° characterised by higher IQ parameter, which can be connected with the formation of subgrains. This is a transient stage of microstructure restoration which at the end leads to the formation of nuclei and growth of recrystallized grains. In such a case, two

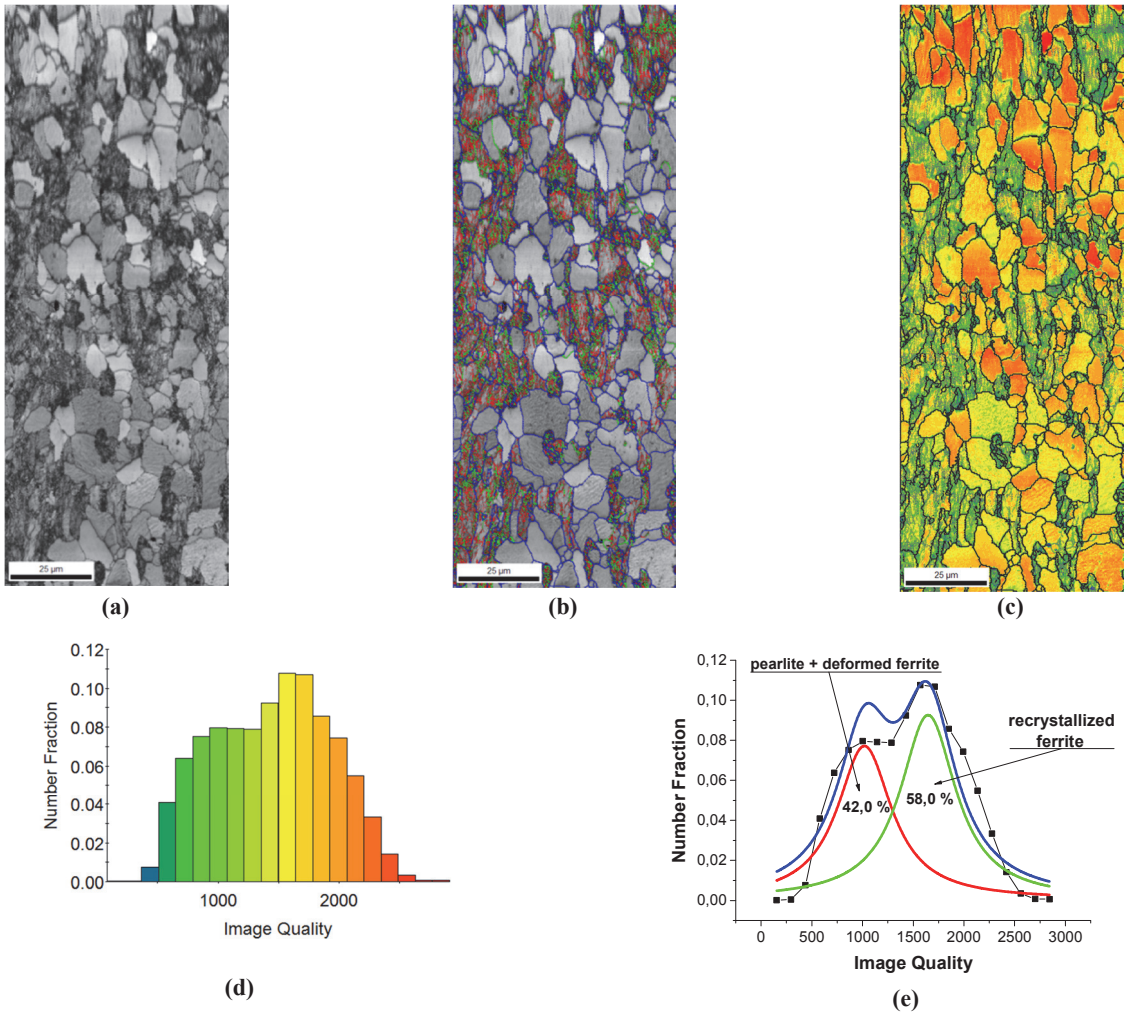

Fig. 5. IQ map of the sample cooled from the peak temperature of 700°C (a) in reference to analyzed map without marked grain/subgrain boundaries (b) and maps with grains/subgrains boundaries (c)

In order to evaluate the fraction of recrystallized grains in the examined area, the deconvolution method of IQ parameter distribution is applied, figure 5.

peaks can be separated in the IQ parameter distribution in figure 5e. Recrystallized ferrite grains and areas with subgrains inside deformed grains show IQ

values ranging from 1200÷2600, figure 5c. IQ parameter value for pearlite and deformed ferrite grains is similar and ranges from 400 to 1200, which enables distinguishing them. Using this information, surface fraction of ferrite subject to recovery and static recrystallization can be measured, and is 58.%. The balance can be attributed to the total fraction of deformed ferrite and pearlite grains. Fraction of recrystallized phases can also be determined using parameters KAM, GAM and GOS, which are based on the values of misorientation angle (Radwański, 2015). The results are compared in figure 6.

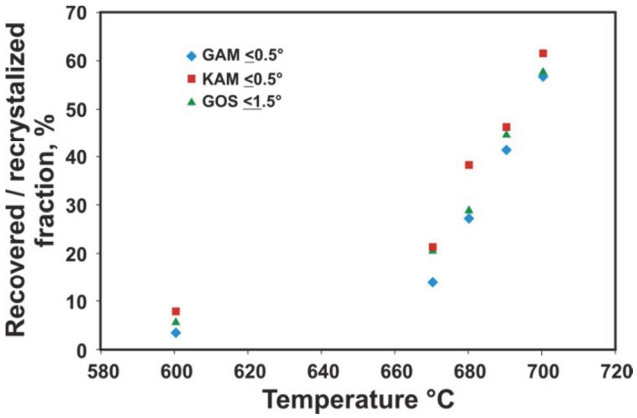

Fig. 6. Fraction of the structure subject to recrystallization measured using different parameters generated in the course of EBSD analysis

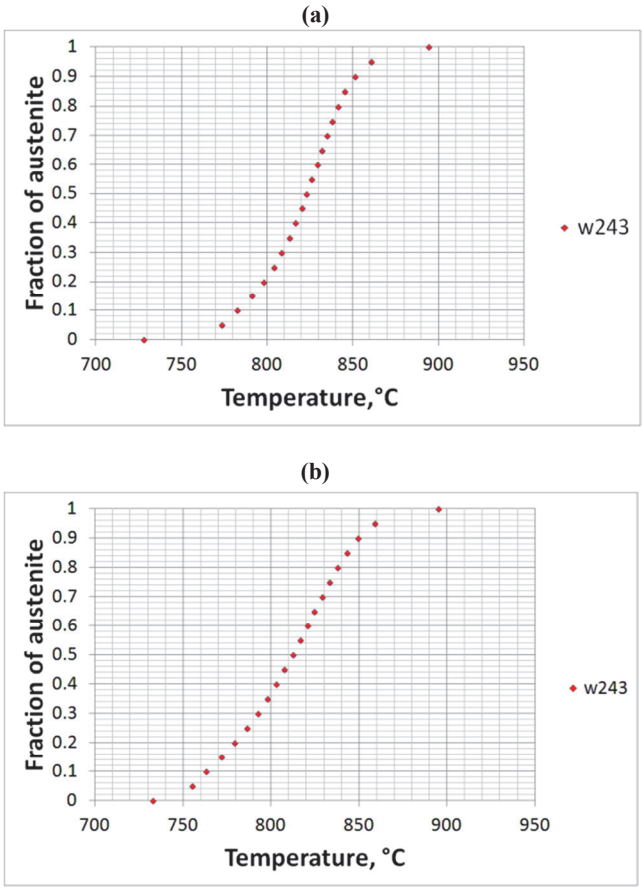

Fig. 7. Changes of austenite volume fraction as function of temperature measured for experimental steel using dilatometry: (a) heating rate 3°C/s; (b) heating rate 10°C/s

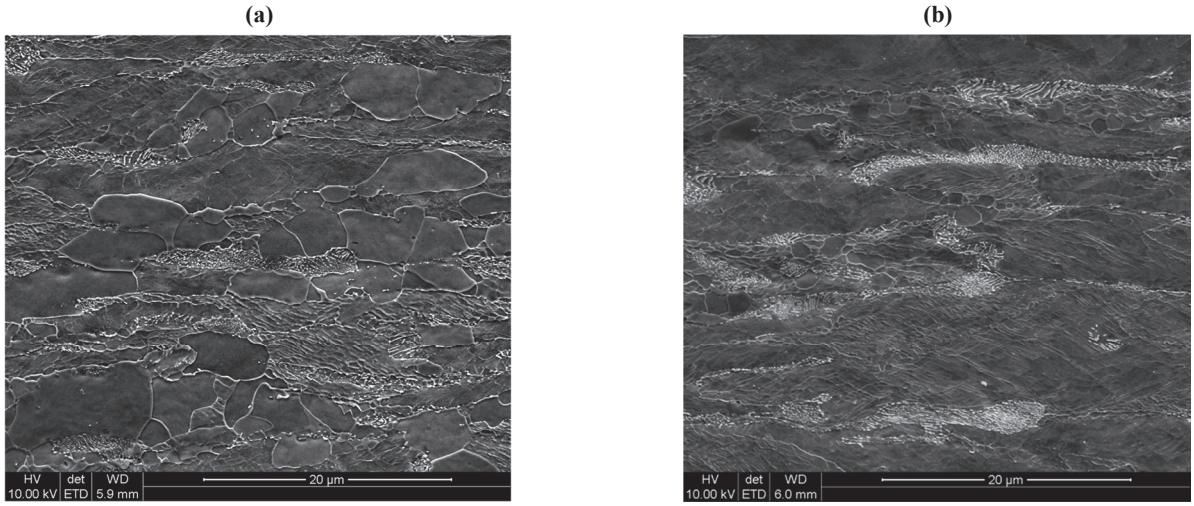

Fig. 8. Comparison of the samples heated to 670 °C at different rates: (a) 3 °C/s; (b) 10 °C/s

The transformation of the cementite particles into austenite starts in the range of 720-750°C which results in the martensite formation during fast cooling following the heating to the maximum temperature (figure 3e). Dilatometric investigation has shown that the transformation to austenite starts in this temperature range and is completed at around 860°C, figure 7.

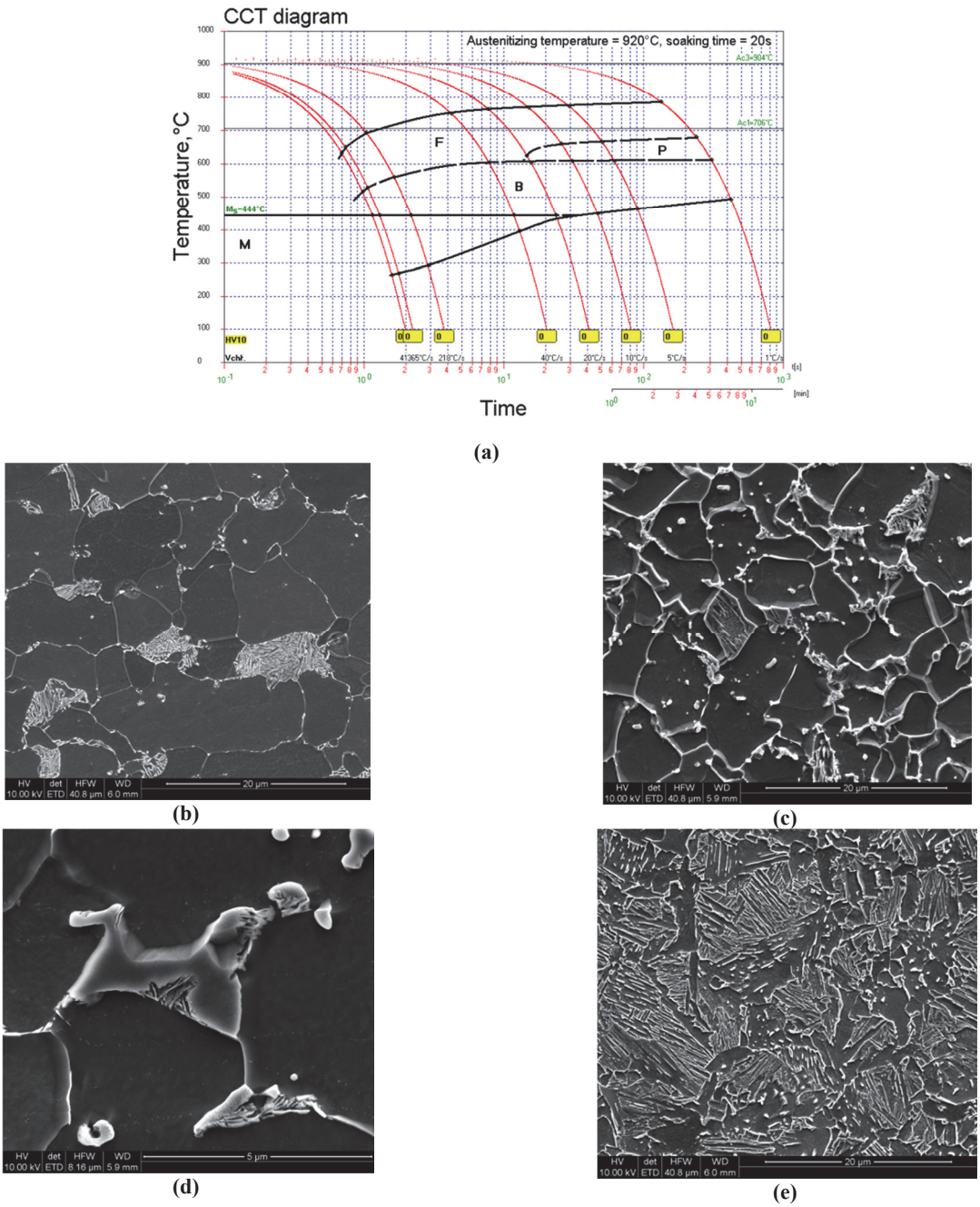

Fig. 9. *CCT diagram (a) and relevant microstrutures obtained after cooling at a rate of: 1 ℃/s (b); 10 ℃/s (c); 20 ℃/s (d); 411 ℃/s (e) after annealing at 920 ℃ for 20 seconds*

Figure 7 shows that there are no substantial differences in kinetics of phase transformation between cooling at a rate of 3 and 10ºC/s. Typically, increasing cooling at a rate of causes shifting transformation start temperatures to higher values. However, increasing heating rate decreases the volume fraction of recrystallized ferrite, figure 8. This means that the transformation of pearlite to austenite during fast heating starts in the not fully recrystallized ferrite which accounts for additional driving force component connected with the stored energy of deformation. This additional term is responsible for accelerating the kinetics of pearlite to austenite transformation.

3.2. Phase transformation during cooling

The information regarding the kinetics of phase transformations as function of cooling rate is essential for designing the continuous annealing thermal profiles for industrial applications. This information on the experimental steel was obtained in the course of dilatometric investigation focused on the CCT diagrams development. The effect of the initial microstructure formed at the heating/soaking stage and

the cooling conditions to ambient temperature were investigated. The initial states of the microstructure prior to cooling include fully austenitic state as well as austenite – ferrite one containing different volume fractions of these constituents. Examples of the results of such an investigation are shown in figures 9 and 10.

tensite is formed in the samples austenitized at 790ºC. On the contrary, in the samples austenitized at 920ºC, the hard constituents contain more bainite than in the samples austenitized at 790ºC. This is connected with differences in carbon content of austenite at both temperatures and is reflected in lower M_s temperature after austenitization at this tempera-

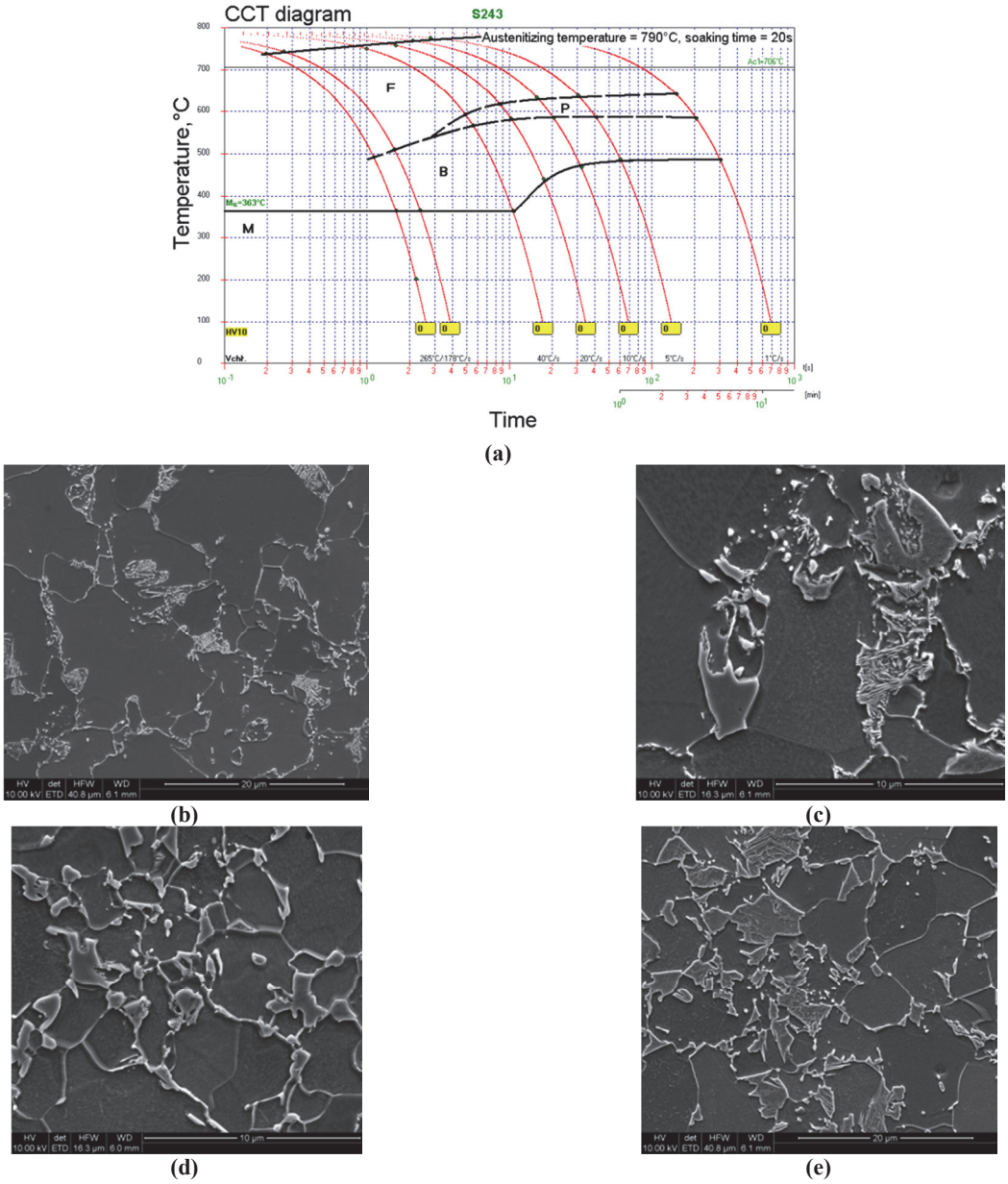

Fig. 10. *CCT diagram (a) and relevant microstrutures obtained after cooling at a rate of: 1 ℃/s (b); 10 ℃/s (c); 20 ℃/s (d); 265 ℃/s after annealing at 790 ℃ for 20 seconds*

Microstructure after austenitization at 920ºC consists only of austenite whilst that soaked at 790ºC contains around 30% of austenite and the rest is ferrite. This means that the austenite formed at 790ºC contained more carbon in solid solution and generally exhibits higher hardenability. Comparing the microstructures in figures 9 and 10, referring to the same cooling rates, one can see that more martensite. However, the increased hardenability of austenite does not slow down substantially the ferrite transformation kinetics. This, in turn, can be associated with the fact that starting transformation from two-phase region does not involve the nucleation state and the new ferrite grows epitaxially on the existing one, which speeds up the progress of transformation.

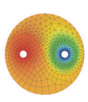

3.3. Relations between thermal profile parameters and mechanical properties

The range of thermal profiles that can be realized in industrial continuous annealing lines is limited by their technical capabilities. Therefore, the final properties of strips are controlled via the interaction among applied thermal profile, strip thickness and strip chemical composition.

The most influential parameters of the thermal profile in continuous annealing process include:

- heating rate;
- peak temperature and soaking time;
- cooling rate after soaking;
- tempering temperature and time.

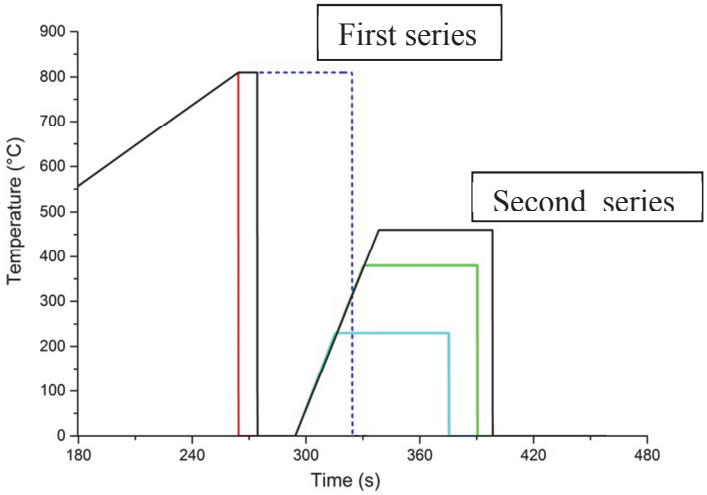

Fig. 11. *Schematic characterization of temperature versus time changes in the performed tests*

In this part of the paper, the effect of the peak temperature, soaking time at peak temperature and tempering temperature/time will be considered as being fundamental for the continuous annealing process. The cold rolled strip samples having width of 55 mm and length of 250 mm were subject to physical simulations of continuous annealing in Gleeble 3800 thermal-mechanical simulator. The simulations were divided into two stages, figure 11. First, the effect of peak temperature and soaking time at this temperature was analyzed. The soaking temperatures 780 and 810°C and soaking times 0 (fast cooling just after reaching peak temperature), 10 and 60 seconds were considered in the experiments. Heating rate to peak temperature was 3°C/s. With this heating rate, the recrystallization of deformed ferrite grains precedes the phase transformation of pearlite into austenite. In the first series of tests, a fast cooling with water was applied after soaking period.

The mechanical properties of the samples after the tests are given in table 2 and the microstructures are shown in figure 12.

Table 2. *Mechanical properties of the samples subject to continuous annealing experiments in Gleeble 3800 simulator*

Annealing	$R_{p0.2}$, MPa	R_m, MPa	A_{gt}, %	A, %	HV0.5
780°C/0s	292	586	13.1	18.9	260
780°C/10s	300	608	12.0	17.1	262
780°C/60s	309	626	11.9	19.3	279
810°C/0s	318	621	11.3	16.4	279
810°C/10s	358	644	10.2	15.2	276
810°C/60s	404	692	10.2	16.5	279

The increase in soaking time at 780°C results in Ultimate Tensile Strength increase while Proof Stress is maintained at approximately the same level. On the contrary, at soaking temperature of 810°C, both Ultimate Tensile Strength and Proof Stress increase as the soaking time increases. This can be explained in terms of the changes occurring in the microstructure of the samples. At both temperatures, increase in soaking time causes an increase in the martensite volume fraction. This is due to the kinetics limits in the pearlite to austenite transformation. However, at peak temperature of 780°C, this does not substantially affect ferrite grain size which explains weak dependence of Proof Stress on the soaking time. At 810°C, increase in martensite volume fraction leads to decrease of ferrite grain size and as a result increase of Proof Stress.

In the second sequence of experiments, the effect of tempering temperature and time was analyzed. The tempering temperatures 230, 380, 460°C and times 60 and 240 seconds were considered in the experiments. Heating rate to tempering temperature was 10°C/s. The mechanical properties of the samples after the tests are given in table 3 and the microstructures are shown in figure 13.

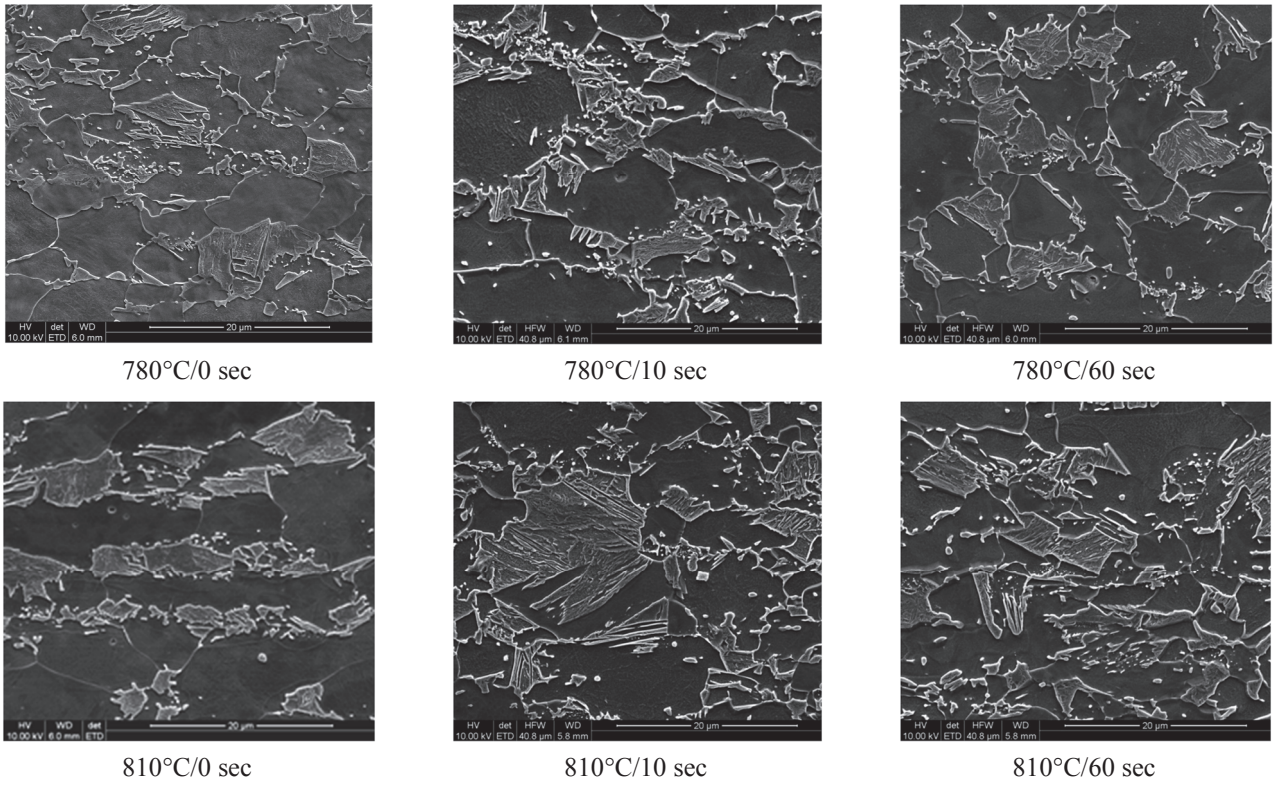

Fig. 12. *Microstructures of the samples subject to the tests in Gleeble 3800 simulator*

Table 3. *Mechanical properties of the samples subject to continuous annealing experiments in Gleeble 3800 simulator*

Soaking	Tempering	$R_{p0.2}$, MPa	R_m, MPa	A_{gt}, %	A, %
780°C/10s	without tempering	300	608	12.0	17.1
	230°C/60s	301	592	13.5	18.6
	230°C/240s	314	581	11.6	17.6
	380°C/60s	375	535	11.9	21.4
	380°C/240s	421	535	10.9	15.6
	460°C/60s	378	506	10.4	17.8
	460°C/240s	389	495	12.2	19.2
810°C/10s	without tempering	358	644	10.2	15.2
	230°C/60s	356	626	10.7	16.6
	230°C/240s	360	625	9.9	19.4
	380°C/60s	436	583	5.4	17.8
	380°C/240s	454	564	7.5	15.8
	460°C/60s	415	546	9.2	15.6
	460°C/240s	423	532	9.9	17.4

Both for samples after soaking at 790 and 810°C, the increase in tempering temperature results in Ultimate Tensile Strength decrease whilst Proof Stress change into Yield Strength with clear yield point and its value increase. The increase in tempering time results in Ultimate Tensile Strength decrease and Yield Strength increase as well. However, the influence of the tempering time on mechanical properties seems to be weaker than that of tempering temperature. The decrease in Ultimate Tensile Strength caused by the increase both temperature and time can be explained by tempering of martensite. And the change from Proof Stress into Yield Strength and the increase of its value might be explained by ageing of ferrite. The microstructure of all samples is composed of ferrite and tempered martensite and are shown in figure 13. Comparing the samples after the same tempering times, one can

observe more advanced process of precipitation and coagulation of iron carbides in the regions of the former martensite.

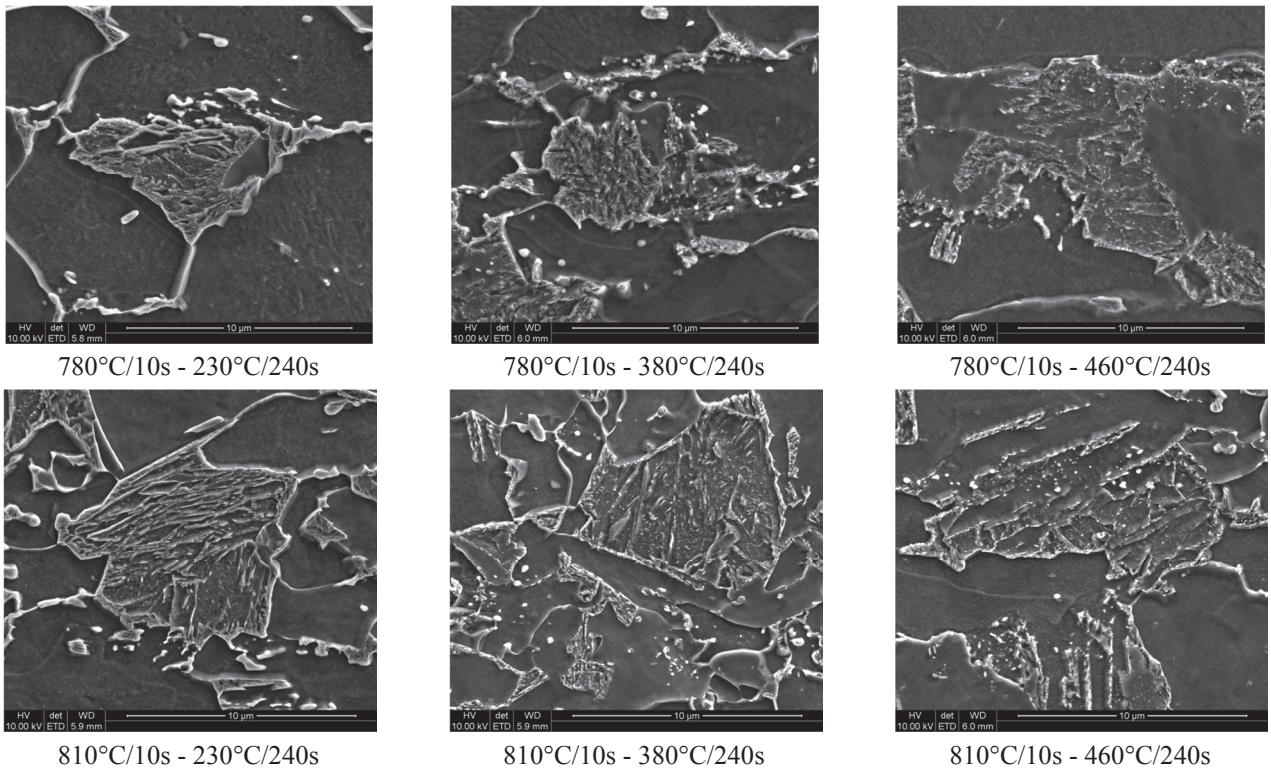

Fig. 13. *Microstructures of the samples subject to tempering*

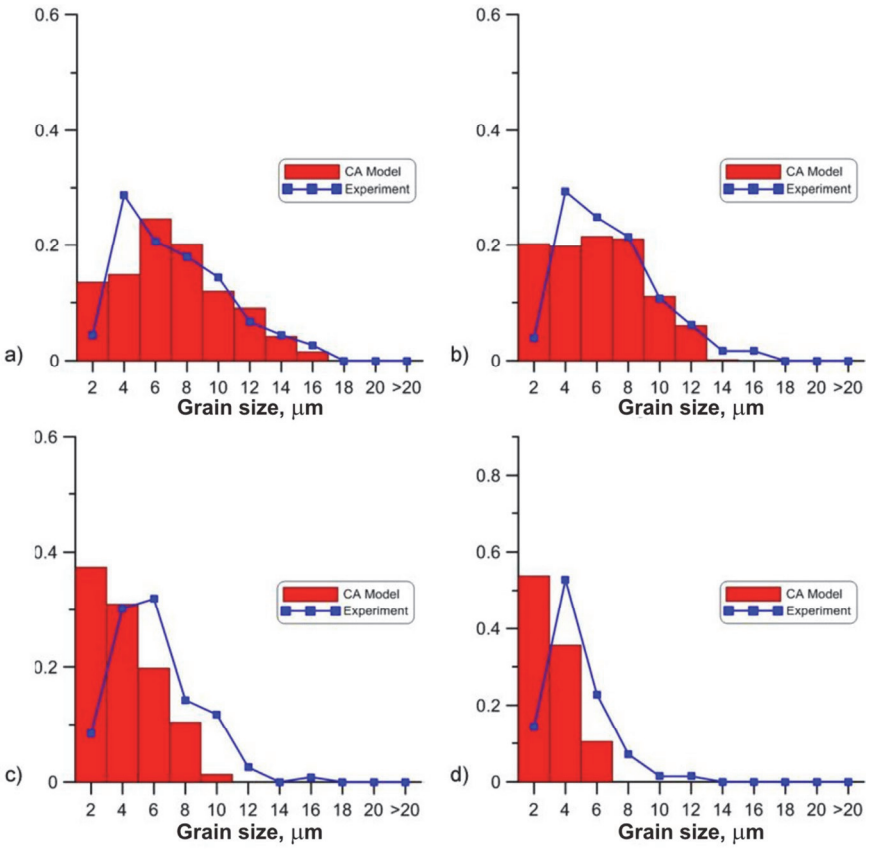

Fig. 14. *Comparison of the grain size distributions obtained experimentally and numerically after heating to 700°C with different heating rates: a) 1, b) 3, c) 5 and d) 8°C/s*

3.4. Example of the application of the obtained results

The quantitative results obtained in the presented investigation were used in the VADPSheet project (Kuziak, 2015) for the development of the conventional and discrete phase transformation models in DP steels during continuous annealing process. Example of the comparison of the results obtained with EBSD analysis and developed Cellular Automata model for static recrystallization of ferrite is shown in figure 14. In this figure, the distribution of ferrite recrystallized grains size measured with EBSD technique is compared with the predicted grain size distribution in the samples subject to heating to 700°C at rates 1, 3, 5 and 8°C. One can see a good correspondence of both distributions. Better agreement between the measured and predicted distribution is obtained at higher grains sizes. This feature can be attributed to the applied magnification during the measurements. The EBSD analysis is a long lasting process, and typically the number of measured microstructural features may not be large enough to accurately characterize the state of the sample.

Using the obtained results, also the phase transformations models during heating and cooling stage of DP steels subject to continuous annealing were developed and their capabilities are presented in (Kuziak, 2015).

4. CONCLUSIONS

1. The start and finish temperature of ferrite recrystallization and austenite formation depends strongly on the heating rate. During slow heating at rate of 3°C/s, ferrite recrystallization starts at around 600°C and is completed at around 750°C. As a result, the structure is completely recrystallized prior to the onset of ferrite + perlite to austenite + ferrite transformation. Increasing the heating rate to around 10°C/s prevents from the ferrite recrystallization prior to the start of phase transformation.
2. A strong interaction of deformed ferrite recrystallization and phase transformation of initial ferrite + pearlite to austenite + ferrite structure was found in the investigation. Due to the additional contribution of deformation energy to the whole Gibbs energy difference due to the transformation, the kinetics of austenite formation are faster when it is formed in the non-recrystallized ferrite environment. This effect counterbalances the effect of heating rate on the phase transformation.
3. The ferrite transformation after soaking stage in the intercritical temperature range starts almost instantaneously after the commencement of cooling. This is due to the lack of ferrite nucleation stage. The "new" ferrite in this case is formed via epitaxial growth on the "old" one. On the contrary, nucleation process occurs when the cooling starts from the temperature of austenite stability. As a result, the microstructure of experimental steel differs substantially when different soaking temperatures are applied.
4. The soaking temperature and time have a strong effect on the relation between Prof Stress and Ultimate Tensile Strength. At lower soaking temperatures (close to Ac_1), increasing soaking time leads to martensite increase without affecting the ferrite grain size after annealing. On the contrary, application of high soaking temperatures (close to Ac_3) results in simultaneous increase in martensite volume fraction and refinement of ferrite grain size. As a result, both Proof Stress and Ultimate Tensile Strength are affected.
5. Further possibility of adjusting the relation between Proof Stress and Ultimate Tensile Strength is connected with the tempering process since application of tempering increases Proof Stress and at the same time decreases Ultimate Tensile Strength. This is important for shaping the use properties of DP steels, such as hole expansion.
6. The application of FEG_SEM and EBSD methods to characterize the metallurgical changes occurring during the laboratory simulations of continuous annealing process enabled the development of capable conventional and Cellular Automata models allowing for the accurate prediction of the effect of processing parameters on DP steels microstructure.

ACKNOWLEDGEMENT

This work was supported by Research Fund for Coal and Steel, Project No. RFSR-CT-2011-00014.

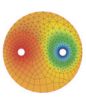

REFERENCES

Aarnst, M., 2009, Microstructural Quantification of Multi Phase Steels - MICRO-QUANT, *RFCS Project No. RFSR-CT-2006-00017*.

Bag, A., Ray, K. K., Dwarakadasa, E.S., 1999, Influence of Martensite Content and Morphology on Tensile and Impact Properties of High-Martensite Dual-Phase Steels, *Metallurgical and Materials Transactions A*, 30A, 1193-1202.

Calcagnotto, M., Ponge, D., Adachi, Y., Raabe, D., 2009, Effect of grain refinement on strength and ductility in dual-phase steels, *Proceedings of the 2nd International Symposium on Steel Science Strength, Plasticity and Fracture in Steels, Fundamentals and Novel Approaches for New Demands*, Kyoto, Japan, 195-198.

Krebs, B., Hazotte, A., Germain, L., Goune, M., 2010, Quantitative Analysis of Banded Structures in Dual-Phase Steels, *Image Anal. Stereol.*, 29, 85-90.

Kuziak, R., Kawalla, R., Waengler, S., 2008, Advanced high strength steels for automotive industry, *Arch. Civ. Mech. Eng.*, 8 (2), 103-117.

Kuziak, R., 2015, Final Report, Property oriented design of hard constituent hardness and morphology in continuously annealed/galvanised DP sheets - VADPSheets, *RFCS Project, No. RFSR-CT-2011-00014*.

Radwanski, K., 2015, Application of FEG-SEM and EBSD Methods for the Analysis of the Restoration Processes Occurring During Continuous Annealing of Dual-Phase Steel Strips, *Steel Research Int.*, 86(11), 1379-1390, DOI: 10.1002/srin.201400361.

Radwański, K., A. Wrożyna, A., R. Kuziak, R., 2015, Role of the advanced microstructures characterization in modeling of mechanical properties of AHSS steels, *Materials Science Engineering*: A, 639, 567-574.

Radwański, K., Wrożyna, A., Kuziak, R., 2015, Role of the advanced microstructures characterization in modeling of mechanical properties of AHSS steels, *Materials Science and Engineering* A, 639, 567-574.

ZMIANY MIKROSTRUKTURALNE I WŁAŚCIWOŚCI MECHANICZNYCH STALI DP W PROCESIE CIĄGŁEGO WYŻARZANIA

Streszczenie

W artykule przedstawiono wyniki badań ukierunkowanych na scharakteryzowanie zmian zachodzących w strukturze stali DP w procesie ciągłego wyżarzania. Do zmian tych zalicza się statyczna rekrystalizacja ferrytu, przemiana wyjściowej ferrytyczno – perlitycznej struktury do struktury ferrytyczno – austenitycznej podczas nagrzewania i wygrzewania oraz przemianę austenitu w ferryt, a następnie w bainit i martenzyt podczas chłodzenia i galwanizowania. Stwierdzono, że rekrystalizacja statyczna ferrytu podczas nagrzewania rozpoczyna się w temperaturze około 600^{o}C, podczas gdy przemiana ferryt +perlit w ferryt + austenit rozpoczyna się w temperaturze około 750^{o}C. Kinetyka przemian fazowych podczas chłodzenia silnie zależy od maksymalnej temperatury cyklu wyżarzania. W przypadku, gdy temperatura ta mieści się w zakresie dwufazowym, obserwuje się epitaksjalny wzrost ferrytu, bez zarodkowania, na "starym" ferrycie. Przemiana ferrytyczna rozpoczyna się wtedy niemal natychmiast po rozpoczęciu chłodzenia. Z kolei, podczas chłodzenia z zakresu stabilności austenitu, przemiana ferrytyczna zachodzi mechanizmem zarodkowania i wzrostu. Obserwuje się wtedy znaczne obniżenie temperatury początku przemiany ferrytycznej poniżej temperatury Ae3, którego wielkość zależy od hartowności stali i od szybkości chłodzenia. W warunkach przemysłowych, możliwości regulowania struktury stali DP poprzez sterowanie szybkością chłodzenia są ograniczone z uwagi na proces galwanizowania. Przede wszystkim niemożliwe jest stosowanie dużych szybkości chłodzenia, co powoduje, że oprócz martenzytu, struktura stali DP zawiera również bainit. Symulacje fizyczne procesu ciągłego wyżarzania przeprowadzone z wykorzystaniem symulatora Gleeble 3800 pokazały, że właściwości mechaniczne stali DP silnie zależą od maksymalnej temperatury profilu temperaturowego oraz od temperatury i czasu starzenia.

Received: August 30, 2015
Received in a revised form: September 2, 2015
Accepted: October 12, 2015